Drying Kinetics of Distillers Wet Grains (DWG)
Under Varying Condensed Distillers Solubles (CDS) and Temperature Levels

Rumela Bhadra,[1] K. Muthukumarappan,[1] Kurt A. Rosentrater,[2,3] and S. Kannadhason[1]

ABSTRACT

Cereal Chem. 88(5):451–458

Distillers dried grains with solubles (DDGS) is a widely used animal feed. But transportation of DDGS is often troublesome because of its stickiness. DDGS is formed by combining condensed distillers solubles (CDS) with distillers wet grains (DWG) and then drying. As a first step toward understanding drying behavior, this study's objective was to investigate batch-drying kinetic behavior of DWG with three CDS addition levels (10, 15, and 20% wb) and three drying-temperature levels (100, 200, and 300°C). Multiple nonlinear mathematical models were used to fit experimental drying data for moisture content versus drying rate. A new comprehensive model was devel-

oped ($R^2 = 0.89$, SEM = 18.60) from a modified Chen and Douglas model to incorporate CDS and drying-temperature terms. Drying temperature affected drying rate more significantly than did changes in CDS level; thus, drying temperature was the main effect and CDS was a subeffect. Increasing the drying temperature increased the drying rate significantly for all levels of CDS addition. This model can be used for predicting DWG drying behavior under broad operating conditions; it can be used to help the industry produce better DDGS, which may thus result in better DDGS handling and transport characteristics.

With the exponential growth of the U.S. fuel ethanol industry in the past decade, large quantities of corn-based distillers dried grains with solubles (DDGS) are now being produced. According to the Renewable Fuels Association (RFA), DDGS production in the United States in 2010 was about 30.5 million metric tons, and the major production of DDGS was from dry-grind ethanol plants (RFA 2010). DDGS typically contains 86–93% (db) dry matter, 26–34% (db) crude protein, and 3–13% (db) fat (Rosentrater and Muthukumarappan 2006). Because of its relatively high amounts of protein and energy, DDGS has been used as livestock feed for both ruminant and nonruminant animals for many years. DDGS also has minerals such as calcium and phosphorus and important amino acids such as methionine, leucine, and so on (Speihs et al 2002). It has been estimated that DDGS consumption has historically been highest in cattle (beef and dairy, 84%), followed by swine (11%) and poultry (5%). Apart from its expanding consumption among the domestic and international markets as livestock feed, new uses (such as fertilizers, aquaculture feed, pet litter, and packaging materials) are also being considered to increase demand for this coproduct (Rosentrater and Muthukumarappan 2006; Bharatan et al 2008).

DDGS users often encounter the problem of particle caking when it is transported in rail cars (Rock and Schwedes 2005). The phenomena of caking and flow often lead to unwanted damage to transportation vessels during unloading because sledgehammers are frequently used to break the agglomerated masses of DDGS to get the product to flow. Some possible factors that could be responsible for caking and flowability problems in DDGS include moisture content, soluble solid content, humidity, temperature, fat, and particle size and shape. The role of DDGS chemical constituents such as carbohydrates, protein, and surface fat on flow behavior have been investigated (Bhadra et al 2009b).

DDGS is produced at ethanol plants by mixing distillers wet grains (DWG) (containing nonfermentable solids) and condensed distillers solubles (referred to as CDS or "syrup" in the industry), which is produced by centrifuging the whole stillage after fermen-

tation and then evaporating the centrifuge stream. After the DWG and CDS are combined, the mixture is then subjected to drying at high temperatures, often having 1000°F inlet and 300°F outlet temperatures (Bhadra et al *in press*). The drying process forms an integral part of DDGS production, and it affects the flow behavior and physical and chemical properties of the DDGS. However, little research has been pursued in terms of quantifying drying behavior.

Drying is a critical process because it has a great effect on the quality of end products (Sharma et al 2003; Kingsly and Singh 2007). The evaluation of drying behavior is important to understanding a host of resulting material properties, such as food taste quality and nutritional value (Zheng and Lan 2007), moisture diffusion coefficient (Tolaba et al 1997), and milling properties (Gibson et al 1998). For example, mathematical models to predict moisture content and drying rate were developed by Madhiyanon et al (2002) (for rice) and Achariyaviriya and Punyabutee (2003) (for fruits). Research on mathematical modeling of drying rate and moisture content was done by Chen and Douglas (1999) with light grades of paper and textiles by air drying processes. In that study, which used established mathematical models for drying rate versus moisture content, three distinct zones for a typical drying rate curve (initialization period [increasing rate period], constant rate period, and falling rate period) were well depicted. The model fitting for the falling rate period was performed with the Churchill and Usagi (1972) model and the power-law model of Chen et al (1995). Finally, an overall comprehensive model that could predict the drying rate curve for all three zones of the curve was established. These types of models help in designing dryers and obtaining optimal process parameters for drying processes.

Over the years, many studies on DDGS production, processing, and characterization have been published. For example, some studies include modeling sorption isotherm (type III isotherm) behavior (Ganesan et al 2008), dynamic water adsorption (Ganesan et al 2009), and material handling characteristics and flowability (Ganesan et al 2007), as well as physical and chemical characterization of commercial samples (Bhadra et al 2009a). But to date, there have been no studies of drying behavior of DDGS. Drying is a key process in the production of DDGS; drying conditions affect the resulting physical properties, which in turn affect the flowability of the DDGS particles. There is currently a substantial lack of knowledge regarding drying characteristics of DDGS and mathematical descriptions of this behavior, and there has been no research done toward understanding the drying kinetics of DDGS. Therefore, our main objective was to establish mathematical drying models for DDGS that can be used to ex-

[1] Graduate research assistant, professor, and graduate research assistant, respectively. Department of Agricultural and Biosystems Engineering, South Dakota State University, Brookings, SD.
[2] Assistant professor, Department of Agricultural and Biosystems Engineering, Iowa State University, Ames, IA.
[3] Corresponding author. Phone: 515-294-4019. Fax: 515-294-6633. E-mail: karosent@iastate.edu

plain drying rate (derived from moisture loss) for various CDS-addition and drying-temperature levels.

MATERIALS AND METHODS

Sample Collection and Sample Preparation

Samples of DWG and CDS were collected from a commercial fuel ethanol plant in South Dakota and were stored frozen ($-10 \pm 1°C$) until experimentation began. For each CDS-DWG combination, CDS was added to DWG at levels of 10%, 15%, and 20% (wb); levels were selected based on our prior work (Bhadra et al 2009a, 2009b, *in press*) and on discussions with industry experts (*unpublished*). The mixture was then blended thoroughly in a laboratory mixer (AUTOMIX model D300, Hobart Corporation, Troy, OH) for 5 min. Each of the CDS-DWG combinations was replicated eight times, yielding 24 (3 × 8) samples, each of which was then subjected to three drying temperatures (thus, $n = 72$ total runs in the study), following a full factorial experimental design. The mixed CDS-DWG samples were placed in plastic bags and stored ($-10°C$) to prevent microbial spoilage of the samples until experimentation began.

Drying Experiments

Approximately 10 g of each of the CDS-DWG replicates was spread uniformly onto a thin steel plate (which had a diameter of 66.6 mm, plate thickness of 0.60 mm, and total surface area of 0.0034 m^2). Samples were dried in a laboratory-scale oven (model 838F, Fisher Scientific, Pittsburg, PA). Drying was done at one of three temperatures (100, 200, or 300°C) for all samples. These temperatures were chosen based on interviews and discussions with various industry experts (data not published). A balance was placed on top of the oven and attached to the sample (with a thin wire cable) to measure changes in sample mass from drying over time, as illustrated in Figure 1. This dynamic process was used to minimize heat loss and maintain the accuracy of the drying data. For the 100 and 200°C drying temperatures, mass changes were recorded every 2 min until three consecutive readings yielded constant mass values. For 300°C, however, the mass was recorded every 1 min because of the faster drying rates at this elevated temperature. After all data were collected, moisture changes were calculated. In Dadali et al (2007), the drying rate was based on the ratio of the change in moisture content to time. But in this study, moisture change was calculated as $\Delta X/\Delta T$ (change in mass/change in time) in % (db), and

drying rate was calculated as $(1/A) \times (\Delta X/\Delta T)$ in g/min/m^2, where A represents the total exposed surface area of the drying plate. Time was measured for all runs in minutes.

Mathematical Modeling of Drying Curves

Modeling of drying rate versus moisture content was pursued in multiple stages. In the first stage, a stepwise regression statistical procedure was performed for the entire (i.e., global) dataset, including all CDS addition levels and drying temperatures. The stepwise regression procedure began by choosing an equation containing the single best X (independent) variable and then attempting to build with subsequent addition of Xs, one at a time, as long as these additions were statistically significant (Table I). The order of term addition was determined by using the partial F-test to select which variable to enter next. The highest partial F-value was compared with a default F-to-enter value. After a variable was added, the newly formed equation was then examined to see if any variable should be deleted by comparing it with an F-to-exit value. After multiple iterations, a complete overall regression equation was established for the required response variable (Y) (Draper and Smith 1998). Moisture content, CDS, and drying temperature were the X variables, and various interactions between drying temperature and CDS, along with higher order terms, were also included. This process enabled us to observe all possible effects in the stepwise regression procedure for this data set.

In the second stage of modeling, a Box-Cox transformation on drying rate (the Y variable) was performed, and then the data were modeled through multiple linear regression. Box-Cox transformation is defined as a type of power transformation performed on the response (Y) variable, and it is always positive in value. The given equations were used in order to transform our response variable, drying rate, for mathematical modeling (Myers 1986):

$$W = \begin{array}{l} (Y^\lambda - 1)/\lambda \text{, for } \lambda \neq 0 \\ \text{or} \\ \ln Y \text{, for } \lambda = 0 \end{array} \qquad (1)$$

where W is the transformation operator. Usually λ is in the range of $[-1, 1]$, or perhaps even $[-2, 2]$ at first, and it may be extended later if necessary (Draper and Smith 1998). For this study, λ values of 2, 0.5, -0.5, -2, and 3 were used (Table II).
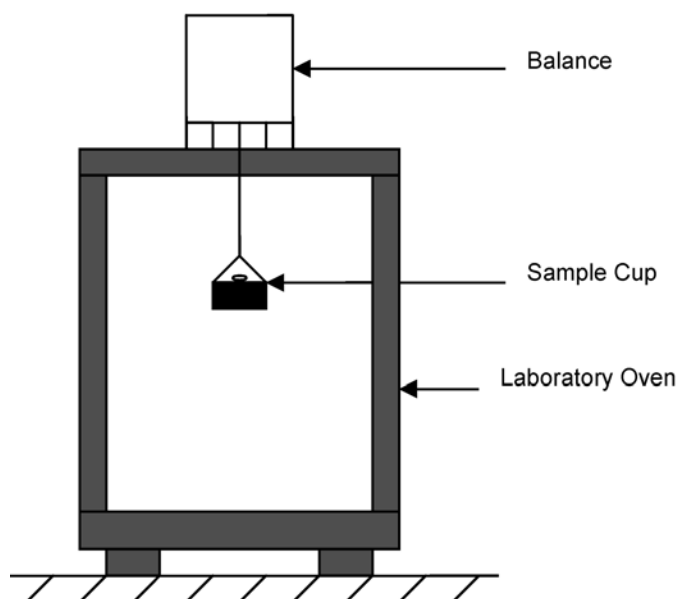

Fig. 1. Schematic of experimental setup used to measure sample mass over time.

TABLE I
Stepwise Multiple Linear Regression Results for Drying Rate vs. Moisture Content for Varying CDS and Drying Temperature Levels, Along with Interaction Terms[a]

Model Term	Parameter Estimates	P-Value
Model results		
Intercept	-0.02	<0.0001
X	-0.78	<0.0001
X^4	2.9E–07	<0.0001
X^5	$-8.9E–10$	<0.0001
$CDS \times Temp \times X$	6.3E–05	<0.0001
$X \times Temp$	0.01	<0.0001
$X^2 \times Temp$	6.3E–05	<0.0001
$X^3 \times Temp$	$-4.51E–08$	<0.0001
$X^2 \times Temp^2$	6.88E–08	<0.0001
Model performance		
Model SS	5,742,687	
Error SS	562,241	
Total SS	6,304,928	
R^2	0.91	
F-statistic	1,526.98	
SEM	21.72	

[a] Drying rate (R) = Σ(model terms); X denotes moisture content (%, db); Temp = drying temperature (°C); CDS = condensed distillers solubles addition level (%, wb); SS = sum of squares; SEM = standard error of the mean; $\alpha = 0.05$ for inclusion; $\alpha = 0.05$ for exclusion.

The next step to modeling drying rate versus moisture content used a semiempirical, semitheoretical approach. Figure 2 represents a typical drying rate versus moisture content curve for biological products; this figure indicates the critical moisture contents, increasing rate period, constant rate period, and falling rate period. According to Chen and Douglas (1999), the drying rate (R) versus moisture content (X) relationship for the increasing rate period is defined as

$$\frac{R}{R_c} = \frac{1 - \exp\{-[h(X)a_p(X)L]/(GC_p)\}}{1 - \exp[-(ha_pL)/(GC_p)]} \tag{2}$$

where R is the instantaneous drying rate (g/min/m^2), R_c is the drying rate constant, X is the instantaneous moisture content (%, db), h is the heat enthalpy of water, G is the drying air-flow rate (m^3/sec), and C_p is the specific heat capacity of water. By defining $n_i = ha_pL/(GC_p)$ and $C = h(Xo)a_p(Xo)/(ha_p)$, then $Ro/R_c = (1 - e^{-n_iC})/(1 - e^{-n_i})$. L, a_p, n_i, and C are the regression constants that will be determined statistically, Ro is the initial drying rate, and Xo is initial moisture content (Chen and Douglas 1999). Approximating equation 2 as $h(X)a_p(X)$, with X as a linear function during the increasing rate period, and approximating $h(X)a_p(X) = ha_p$, $R = R_c$ at $X = Xc_2$, and $R = Ro$ at $X = Xo$, then

$$\frac{R}{R_c} = \frac{1 - e^{-n_i[C + (1-C)(Xo-X)]/(Xo-Xc_2)}}{1 - e^{-n_i}} \tag{3}$$

Equation 3 is thus the simplified form of the increasing rate period (equation 2), where Xc_2 is the second critical moisture content at which the increasing rate period (initialization period) changes to the constant rate period, and Xo is the initial moisture content. If the initial moisture content is very high (as it was found in this study) and if $Ro/R_c \rightarrow 0$ as $C \rightarrow 0$, then equation 3 can be further reduced to

$$\frac{R}{R_c} = \frac{1 - e^{-n_i(Xo-X)/(Xo-Xc_2)}}{1 - e^{-n_i}} \tag{4}$$

Equation 4 represents the final reduced description of the increasing rate period, which shows that R increases exponentially as X decreases; Xc_2, Xo, n_i, and R_c must be determined statistically based on the particular drying conditions.

After the sample mass has reached steady-state drying conditions, that segment of time known as the constant drying rate period occurs. The drying rate is approximately constant as moisture evaporates from the surface of the sample. At some point, the drying will become rate-limited, and the drying rate will begin to decrease. Thus, for the constant rate period, $R = R_c$.

The first critical moisture content is denoted by Xc_1 and is defined as the moisture content at which the constant rate period changes to the falling rate period. A power-law relation for the falling rate period in the drying curve was found to be appropriate by Chen et al (1995) and is given as

$$\frac{R}{R_c} = (X/Xc_1)^{n_f} \tag{5}$$

However, equation 5 has problems during the transition from the constant rate region to the falling rate period (i.e., at Xc_1), as this equation creates an abrupt, unsmooth transition. In addition, the simple power law as given in equation 5 is nonlinear immediately below the first critical moisture value and has maximum curvature as $X \rightarrow 0$. For this power law (equation 5) to adequately represent the falling rate period data, it is necessary to reverse the order of the curved and nonlinear sections by replacing X/Xc_1 and R/R_c with $1 - X/Xc_1$ and $1 - R/R_c$, respectively (Chen and Douglas 1999), which results in the following modified equation:

$$\frac{R}{R_c} = 1 - (1 - X/Xc_1)^{n_f} \tag{6}$$

where Xc_1 is the first critical moisture content (%, db), R is the drying rate (g/min/m^2), and n_f is a regression parameter to be determined statistically. $\Delta R/\Delta X = 0$ at $X = Xc_1$, and thus the falling rate period modeled by equation 6 approaches the constant rate period asymptotically (Chen and Douglas 1999), which is appropriate.

An overall comprehensive drying model was developed by Chen and Douglas (1999) for all three drying rate zones. The ba-
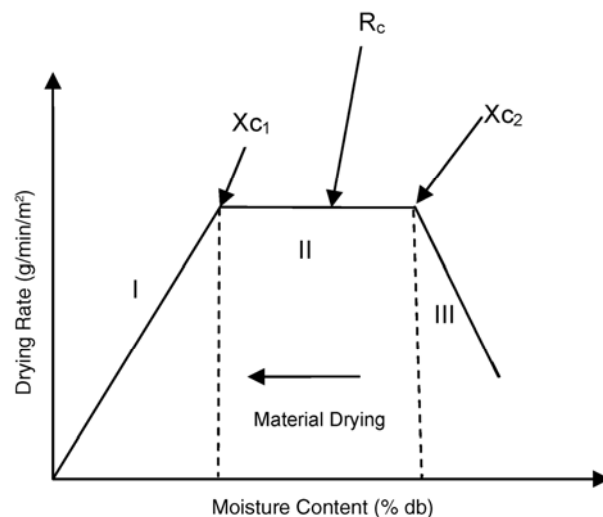

Fig. 2. Typical drying rate vs. moisture content behavior. Transitions between drying periods are denoted by critical points. Drying rate is a function of moisture content; as the material dries, the drying rate travels to the left (i.e., toward the origin). I = falling rate period; II = constant rate period; III = increasing rate (initialization) period; Xc_1 = first critical moisture content (%, db); Xc_2 = second critical moisture content (%, db); and R_c = drying rate, which is approximately constant (g/min/m^2).

TABLE II
Box-Cox Transformation and Linear Regression Results for Drying Rate vs. Moisture Content for Varying CDS and Drying Temperature Levels[a]

		Parameter Estimates				Model Performance					
No.	λ	Intercept	ln X	CDS	Temp	Model SS	Error SS	Total SS	R^2	F-Statistic	SEM
1	2	−28,983.3	3,986.6	39.05	91.91	4.75E+10	2E+10	66,339,591,634	0.58	559.83	6,352
2	3	−4,795,954.0	623,845	14,871.72	14,454.85	1.64E+15	7E+14	2.35662E+15	0.41	278.97	1E+06
3	0.5	−23.37	4.96	−0.02	0.08	66,683.36	15,508	82,191.09	0.81	1,722.87	3.68
4	−0.5	0.25	0.24	−0.003	0.002	91.33	150.2	241.57	0.38	243.41	0.62
5	−2	0.27	0.04	−0.001	0.0002	2.50	19.91	22.41	0.11	50.3	0.13

[a] Drying rate (R) = Σ(model terms); Box-Cox transformation is $W = (Y^\lambda - 1)/\lambda$ for $\lambda \neq 0$, or $W = \ln Y$ for $\lambda = 0$. X denotes moisture content (%, db); CDS = condensed distillers solubles addition level (%, wb); No. = transformation number; Temp = drying temperature (°C); SS = sum of squares; and SEM = standard error of the mean. P-values for all parameter estimates were found to be <0.0001.

sic models used for fitting drying rate and moisture content data and the ranges of validity are reiterated in equations 7, 8, and 9, for the increasing rate period (initialization period), constant rate period, and falling rate period, respectively:

$$\frac{R}{R_c} = \frac{1 - \exp\left[-n_i(Xo - X)/(Xo - Xc_2)\right]}{1 - \exp(-n_i)} \quad \text{for } Xo > X > Xc_2 \quad (7)$$

$$\frac{R}{R_c} = 1 \quad \text{for } Xc_2 > X > Xc_1 \quad (8)$$

$$\frac{R}{R_c} = 1 - \left(1 - X/Xc_1\right)^{n_f} \quad \text{for } Xc_1 > X > 0 \quad (9)$$

where R is the instantaneous drying rate (g/min/m^2), R_c is the drying rate constant (g/min/m^2), X is the instantaneous moisture content (%, db), Xo is the initial moisture content (%, db), Xc_2 is the second critical moisture content (%, db) at which the increasing rate period changes to the constant rate period, Xc_1 is the first critical moisture content (%, db) at which the constant rate period changes to the falling rate period. Thus, Xc_2, Xc_1, n_f, n_i, and R_c must be determined statistically.

Our goal was not just to quantify drying rate as a function of moisture content but also to include CDS addition and drying temperature effects in order to establish an overall comprehensive model for DDGS drying. To achieve this overall model, various permutations and combinations of equations 7, 8, and 9 were used

(based on Chen and Douglas 1999). Table III represents the various modified equations used.

Statistical Analysis

Parameter estimates for the above models were determined with nonlinear regression through the PROC NLIN procedure in SAS version 9.1 (SAS Institute, Cary, NC), which used the Gauss-Newton method to resolve the models and predict the parameter estimates. Gauss-Newton is the most common method used for nonlinear modeling (Seber and Wild 1989). PROC NLIN directly gave the F-statistic (or F-value) and R^2 values, which were calculated from the model sum of squares, total sum of squares, and error sum of squares. The standard error of the mean (SEM) for each of the models was

$$\text{SEM} = \sqrt{\frac{\sum(Y_i - \hat{Y}_i)^2}{DF}} \quad (10)$$

where Y_i and $\hat{Y}_i$ are the experimentally observed and predicted drying rates, respectively, and DF is the degree of freedom (number of data points minus the number of coefficients in the model).

The suitability of each model in this study was determined by comparing the SEM, F-statistic, coefficient of determination (R^2), parameter estimate values, and residual plots. A survey of the literature on drying revealed that these parameters were most often used to compare models (Sharma et al 2003; Sogi et al 2003; Wang et al 2004; Domyaz 2005; Menges and Ertekin 2006). Some have also

TABLE III
Global Equations Used for Nonlinear Modeling of Drying Rate (R) = f(Moisture Content, X) for Varying CDS and Drying Temperature Levels[a]

No.	Falling Rate Period	Constant Rate Period	Increasing Rate (Initialization) Period
G1	$R_c \times [1-(1-X/Xc_1)^{n_f}] + b1 \times CDS \times T$	$R_c + b1 \times CDS \times T$	$R_c \times \{1-\exp[-n_i \times (Xo-X)/(Xo-Xc_2)]\}/[1-\exp(-n_i)] + b1 \times CDS \times T$
G2	$R_c \times [1-(1-X/Xc_1)^{n_f}] + b1 \times CDS + b2 \times T$	$R_c + b1 \times CDS + b2 \times T$	$R_c \times \{1-\exp[-n_i \times (Xo-X)/(Xo-Xc_2)]\}/[1-\exp(-n_i)] + b1 \times CDS + b2 \times T$
G3	$R_c \times [1-(1-X/Xc_1)^{n_f}] + b1 \times CDS + \exp(b2 \times T)$	$R_c + b1 \times CDS + \exp(b2 \times T)$	$R_c \times \{1-\exp[-n_i \times (Xo-X)/(Xo-Xc_2)]\}/[1-\exp(-n_i)] + b1 \times CDS + \exp(b2 \times T)$
G4	$R_c \times [1-(1-X/Xc_1)^{n_f}] + b1 \times \exp(b2 \times CDS \times T)$	$R_c + b1 \times CDS + b2 \times T$	$R_c \times \{1-\exp[-n_i \times (Xo-X)/(Xo-Xc_2)]\}/[1-\exp(-n_i)] + b1 \times \exp(b2 \times CDS \times T)$
G5	$R_c \times [1-(1-X/Xc_1)^{n_f}] + b1 \times \exp(b2 \times CDS \times T)$	$R_c + b1 \times \exp(b2 \times CDS \times T)$	$R_c \times \{1-\exp[-n_i \times (Xo-X)/(Xo-Xc_2)]\}/[1-\exp(-n_i)] + b1 \times \exp(b2 \times CDS \times T)$
G6	$R_c \times [1-(1-X \times T/Xc_1)^{n_f}] + b1 \times CDS$	$R_c + b1 \times CDS \times T$	$R_c \times \{1-\exp[-n_i \times (Xo-X \times T)/(Xo-Xc_2)]\}/[1-\exp(-n_i)] + b1 \times CDS$
G7	$R_c \times [1-(1-X \times CDS/Xc_1)^{n_f}] + b1 \times T$	$R_c + b1 \times CDS \times T$	$R_c \times \{1-\exp[-n_i \times (Xo-X \times CDS)/(Xo-Xc_2)]\}/[1-\exp(-n_i)] + b1 \times T$
G8	$R_c \times [1-(1-X/Xc_1)^{n_f}] + (b1 \times T)/CDS$	$R_c + (b1 \times T)/CDS$	$R_c \times \{1-\exp[-n_i \times (Xo-X)/(Xo-Xc_2)]\}/[1-\exp(-n_i)] + (b1 \times T)/CDS$
G9	$R_c \times [1-(1-X/Xc_1)^{n_f}] + (b1 \times CDS) + b2 \times (T)^{b3}$	$R_c + (b1 \times CDS) + b2 \times (T)^{b3}$	$R_c \times \{1-\exp[-n_i \times (Xo-X)/(Xo-Xc_2)]\}/[1-\exp(-n_i)] + (b1 \times CDS) + b2/(T)^{b3}$
G10	$R_c \times [1-(1-X/Xc_1)^{n_f}] + (b1 \times CDS) + b2 \times (T)^{b3}$	$R_c + (b1 \times CDS) + b2 \times (T)^{b3}$	$R_c \times \{1-\exp[-n_i \times (Xo-X)/(Xo-Xc_2)]\}/[1-\exp(-n_i)] + (b1 \times CDS) + b2 \times (T)^{b3}$

[a] Equations for calculating R, the drying rate (g/min/m^2) at a given point in time, based on Chen and Douglas (1999). X = observed moisture content (%, db) at a given time; CDS = condensed distillers solubles addition level (%, wb); R_c = drying rate constant (g/min/m^2); Xc_1 = first critical moisture content (%, db); Xc_2 = second critical moisture content (%, db); Xo = initial moisture content (%, db); T = drying temperature (°C); n_i, n_f, b1, b2, and b3 are empirical parameter estimates that must be determined statistically.

TABLE IV
Global Nonlinear Regression Results for Modeling of Drying Rate vs. Moisture Content for Varying CDS Levels and Drying Temperatures[a]

Equation No.	Parameter Estimates[b]						Model Performance					
	R_c	n_i	n_f	b1	b2	b3	Model SS	Error SS	Total SS	R^2	F-Statistic	SEM
G1	43.80	–2.76	0.92	0.02			7,259,740	3,188,764	10,448,503	0.69	657.96	45.90
G2	72.75	17.55	1.18	–4.75			8,362,079	2,086,424	10,448,503	0.80	0.52	4,512.02
G3	FTC											
G4	–77.22 (0.358)	10.00	1.00	0.79	1.00		1,223,233	72,384	1,295,617	0.94	1,867.36	785.57
G5	FTC											
G6	–31.33 (0.789)	10.00	–0.03	0.05			2,517,655	382,033	2,899,687	0.87	511.40	56.90
G7	–30.78 (0.841)	10.00	–0.07	0.54			2,535,567	402,379	2,937,945	0.86	730.40	145.56
G8	41.35	–1.11	1.02	3.88			7,242,944	3,205,559	10,448,503	0.69	652.99	171.89
G9	93.45	71.33	5.87	0.43	–27.21	–0.09	5,816,899	4,631,604	10,448,503	0.56	241.55	81.24
G10	**88.12**	**10.49**	**0.43**	**–4.57**	**0.0002**	**0.10**	**9,454,166**	**1,594,337**	**10,448,503**	**0.90**	**2,068.12**	**21.48**
G10a (100°C)	**37.14**	**22.26**	**0.78**	**0.27**	**–0.04**	**1.00**	**78,760**	**41,398**	**89,159**	**0.88**	**207.66**	**18.60**
G10a (200°C)	**128.43**	**37.42**	**3.53**	**–0.44**	**–0.06**	**1.30**	**541,201**	**84,945**	**616,147**	**0.88**	**721.23**	**18.60**
G10a (300°C)	**312.16**	**4.12**	**3.58**	**2.11**	**–0.30**	**1.00**	**1,957,146**	**526,645**	**2,183,791**	**0.90**	**274.80**	**18.60**

[a] See Table III for model equations; R_c, n_i, n_f, b1, b2, and b3 are the empirical parameter estimates for the model terms; SS = sum of squares; SEM = standard error of the mean; FTC = failed to converge. Bold font indicates the final selected optimal model. G10a is the same as G10, but parameter estimates were found for individual drying temperatures (100, 200, and 300°C), separately.

[b] P-values are indicated in parentheses. If no P-value is indicated for a parameter estimate, $P < 0.0001$.

used the chi-square test, adjusted R^2, percentage of variance, and other various statistical tests to evaluate models (Domyaz 2005; Simal et al 2005). In this study, a model was considered "good" if it yielded high R^2 and F-statistic values, relatively small SEM values, reasonable parameter estimate values, and random residual plots and, most important, if it provided a good fit to the actual data.

RESULTS AND DISCUSSION

Table I shows the summary results of the stepwise multiple linear regression for drying rate as a function of moisture content, CDS addition level, and drying temperature. These results encompass the interaction effects of CDS, drying temperature, and mois-

ture content rather than only moisture content and drying temperature effects as did Rosentrater et al (1999). These stepwise regression results serve as an overall global model to predict drying rate as a function of moisture content, CDS addition level, and drying temperature. Table I clearly demonstrates that this procedure yielded an R^2 value of 0.91 and SEM of 21.72, which is very close to our subsequent semiempirical modeling results. However, stepwise regression models are highly dependent on the nature of the dataset used, so the specific form of the resulting model equations may change as the experimental dataset changes, even if the same type of biological samples are used. In addition, the stepwise regression equation is complicated, and hence, it may be troublesome to use in future calculations. Semiempirical,
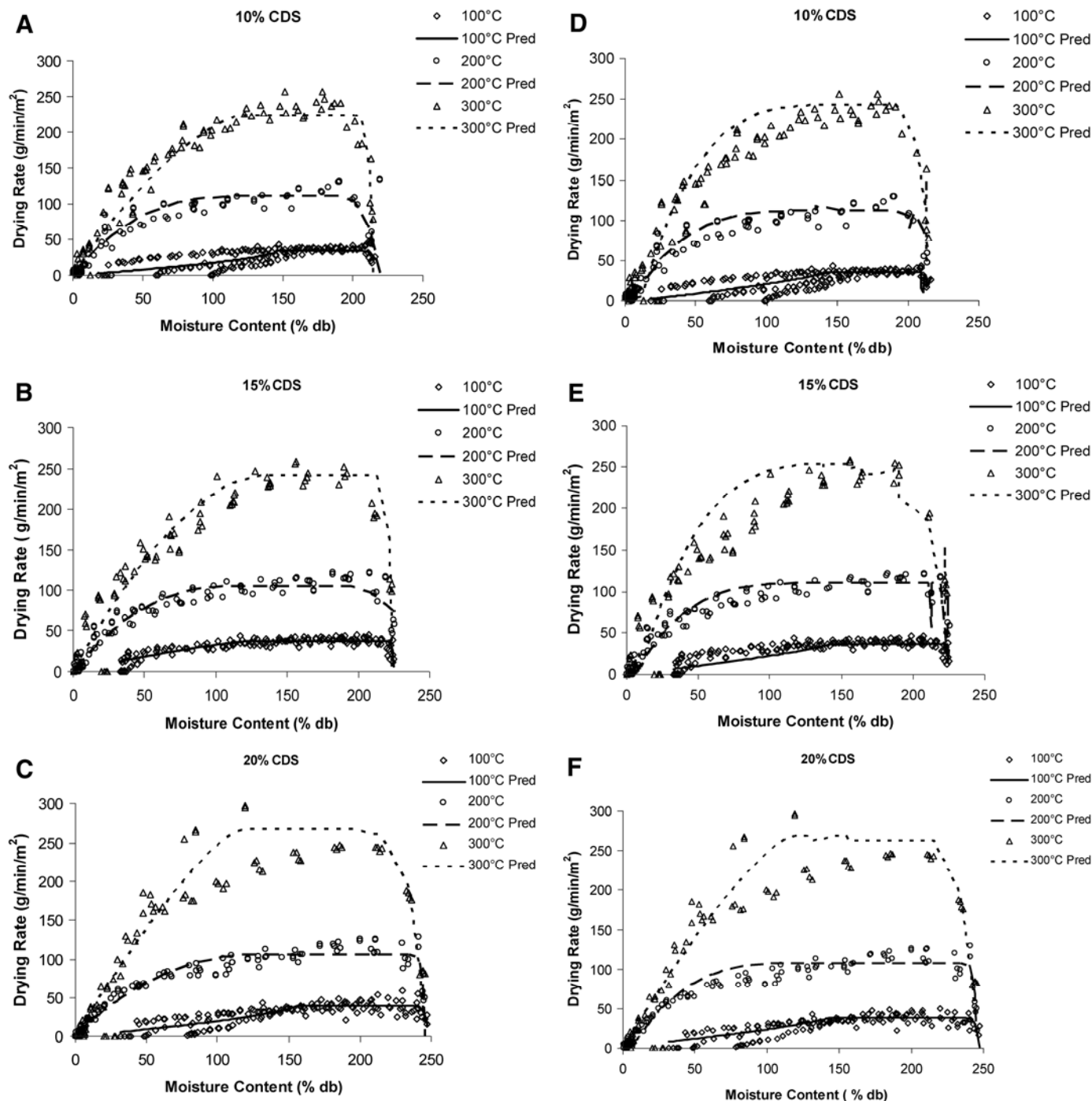

Fig. 3. A–C, Plots of drying rate vs. moisture content predicted by equations 7, 8, and 9 (Chen and Douglas 1999) for each condensed distillers solubles (CDS) and temperature level combination individually. **D–F,** Plots of drying rate vs. moisture content predicted by equation G10 from Table III, which is a modified Chen and Douglas equation and was the single best global equation for all CDS level and temperature combinations simultaneously.
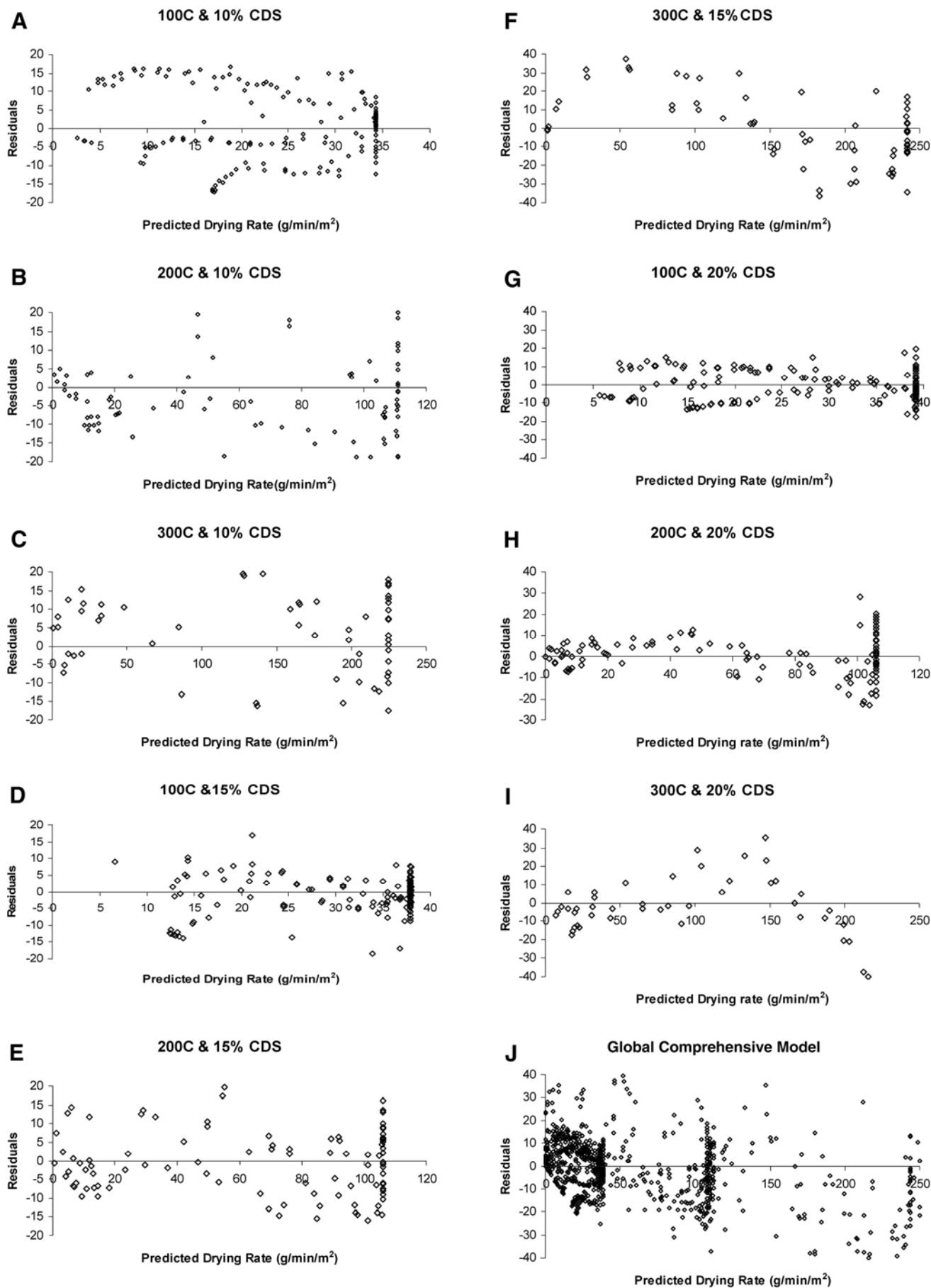
Fig. 4. Residual plots of optimum drying rate models. **A–I,** Chen and Douglas (1999) model (equations 7, 8, and 9): R_c = 34.33, n_f = 0.603, and n_i = 10.122. **J,** Modified Chen and Douglas (1999) model, equation G10, Table III: R_c = 88.12, n_f = 0.43, n_i = 10.49, b1 = –4.57, b2 = 0.0002, and b3 = 0.10 (all the parameter estimates can be found in Table IV).

semitheoretical modeling, which is based on certain assumptions and mathematical theory, tends to have less complicated, more elegant descriptions of drying kinetics. It can also provide unique solutions that can be used under varying operating conditions and are readily amendable to further calculations.

Table II gives the summary of the Box-Cox transformation statistical modeling with different λ values. This approach yielded relatively lower R^2 values (0.11–0.81) and higher SEM values compared with stepwise regression or the subsequent semiempirical modeling (Tables I and IV, respectively). Also, for moisture contents lower than 5% (db), some negative drying rate values were predicted. Thus, Box-Cox transformation was deemed inappropriate for drying of DDGS.

Table III presents all of the modified theoretical-empirical equations used for global modeling of drying rate, and Table IV summarizes the statistical output for all of these global models produced with PROC NLIN that incorporate CDS and temperature as factors. A global comprehensive model was established by modifying the basic equations (7, 8, and 9) drawn from Chen and Douglas (1999), including the increasing rate, constant rate, and falling rate periods, respectively. Model G10, as shown in Table IV, yielded a low SEM value (21.48), high F-value (2068.12), and R^2 of 0.90. Chen and Douglas (1999) used only one independent variable (moisture content), but in our G10 model, CDS addition rate and drying temperature were accounted for as well. Consequently, G10 was deemed most suitable of all models examined in this study.

The G10a models represent the same mathematical model as G10 but vary slightly in modeling strategy. In G10a, R_c values were kept fixed and were inserted into the model equations for 100, 200, and 300°C separately (not simultaneously as for G10). Also, in model G10a, the statistical analysis was done separately for 100, 200, and 300°C drying temperatures; it represented drying rate as a function of varying CDS levels and drying temperatures. Model G10a yielded an overall SEM of 18.60, which is slightly lower than that of model G10. Model G10a did a better job than model G10 because fixing R_c values helped in giving better n_i, n_f, b1, b2, and b3 parameter estimates for each specific drying temperature.

Figures 3A–C show model plots for the predicted drying rate according to Chen and Douglas (1999) base model equations, which do not encompass CDS or drying temperature effects; Figures 3D–F show model plots for predicted drying rate according to model G10 (the overall global model), which included CDS and drying temperature effects. From the drying rate curves for the DDGS samples, a typical drying rate pattern as predicted by Chen and Douglas (1999) can be observed. There were definite increasing rate (warm-up), constant rate, and falling rate periods in the data. The increasing rate period was recognized by Polat (1989), who found that nearly 50% of the moisture was removed during this period. Previous research by Law et al (2003) at drying temperatures of 60–120°C found the presence of a second falling rate after the first falling rate and predicted that the second falling rate was a diffusion-controlled period that was exponentially related to the moisture content. Such a pattern in the DDGS drying rate curves was not observed in these samples. It was observed from Figure 3 that there was only one falling rate period for all CDS levels and drying temperatures.

The drying temperature clearly affected the drying rate for the DDGS, as shown in Figure 3; there was an increase in the drying rate values as the drying temperature increased. By carefully observing the experimental data set for each CDS level (10, 15, and 20%), it can be seen that, as the CDS addition level was increased from 10 to 15%, there was a slight increase in the initial moisture content value, and for the 20% CDS level, the initial moisture content was highest and close to 250% (db).

Comparing Figures 3A and 3D for the 10% CDS level, we see that there was some overprediction at 300°C for moisture content below 100% (db), and a similar drying behavior was ob-

served for 15% CDS. Because the equations used in Figure 3A did not include the CDS and temperature variables (only the base equation of Chen and Douglas [1999] was used), the predicted behavior slightly differed from that in Figure 3D–E for 10 and 15% CDS, for which the global comprehensive model was used to predict the values. It can be seen that drying temperature had a greater impact on drying rate (response variables) than did variation in CDS levels (Figure 3). Thus, temperature was the most important effect for drying rate versus moisture content, and CDS was a subeffect.

Figures 4A–I present residual plots of predicted drying rate according to the optimum model for each treatment combination. The residuals were calculated by subtracting the predicted drying rate values from observed ones (Draper and Smith 1998). There was a fairly random distribution of the residuals along the x-axis in most cases; the relatively even distribution of residuals on either side of the x-axis ($y = 0$) as well indicated that the base model fit the drying rate data fairly well. It is evident that there was an increase in the predicted drying rate as the drying temperature increased from 100 to 300°C, which matched the observed drying rate values depicted in Figure 3. But changing the CDS level did not affect the predicted drying rate as much as did temperature. Figure 4J represents the global model (G10, Tables III and IV) residuals, which showed random distribution, suggesting that the optimal model did not violate the regression assumptions and that it fit observed drying rate data very well. Therefore, selection of the global models (G10 and G10a) is justified and can provide prediction of drying rate values under the CDS levels and drying temperatures used in this study.

CONCLUSIONS

Mathematical models for predicting drying kinetics of DWG into DDGS, with three CDS addition levels (10, 15, and 20% wb) and three drying temperatures (100, 200, and 300°C), were developed. Comprehensive models for drying rate versus moisture content (drawn from the basic Chen and Douglas model) were found to be effective in predicting drying rate, but model performance was augmented when the effects of CDS and drying temperature levels were added. Drying temperature was the most important factor that impacted drying rate, whereas CDS level was less important. The highest drying temperature (300°C) yielded the highest drying rates (~250 g/min/m²). This first step toward understanding the drying of DWG into DDGS can subsequently be used to develop laboratory-scale drying simulation experiments and will ultimately be useful for predicting drying behavior of DDGS. Because no existing models or drying simulation studies have yet been performed for DDGS, this study is a step toward such research areas. Future studies with higher CDS levels and different drying temperature levels should be examined as well. Also, it should be kept in mind that these proposed models are based on a batch convection oven drying process. Hence, future steps should include using a rotary drum dryer for drying experiments and then formulating appropriate models for drying kinetics.

LITERATURE CITED

Achariyaviriya, A., and Punyabutee, T. 2003. Drying kinetics of longan fruit without stone. International Conference on Crop Harvesting and Processing, Louisville, Kentucky, 9–11 February 2003. Am. Soc. Agric. Biol. Eng.: St. Joseph, MI. Available at http://www.energy-

based.nrct.go.th/Article/Ts-3%20drying%20kinetics%20of%20
longan%20fruit%20without%20stone.pdf.

Bhadra, R., Muthukumarappan, K., and Rosentrater, K. A. 2009a. Flow-ability properties of commercial distillers dried grains with solubles (DDGS). Cereal Chem. 86:170-180.

Bhadra, R., Rosentrater, K. A., and Muthukumarappan, K. 2009b. Cross-sectional staining and surface properties of DDGS particles and their influence on flowability. Cereal Chem. 86:410-420.

Bhadra, R., Rosentrater, K. A., Muthukumarappan, K., and Kannadhason, S. *In press*. Desorption studies of DDGS under varying CDS and drying temperature levels. Appl. Eng. Agric.

Bharatan, M., Schingoethe, D. J., Hippen, A. R., Kalscheur, K. F., Gibson, M. L., and Karges, K. 2008. Conjugated linoleic acid increases in milk from cows fed condensed corn distillers solubles and fish oil. J. Dairy Sci. 91:2796-2807.

Chen, G., and Douglas, W. J. M. 1999. Quantification of through drying rate data. Drying Technol. 17:1707-1723.

Chen, G., Gomes, V. G., and Douglas, W. J. M. 1995. Impingement drying of paper. Drying Technol. 13:1331-1344.

Churchill, S. W., and Usagi, R. 1972. A general expression for the correlation of rates of transfer and other phenomena. AIChE J. 18:1121-1128.

Dadali, G., Demirhan, E., and Ozbek, B. 2007. Microwave heat treatment of spinach: Drying kinetics and effective moisture diffusivity. Drying Technol. 25:1703-1712.

Domyaz, I. 2005. Drying behavior of green beans. J. Food Eng. 69: 161-165.

Draper, N. R., and Smith, H. 1998. Applied Regression Analysis. Wiley: New York.

Ganesan, V., Rosentrater, K. A., and Muthukumarappan, K. 2007. Dynamic water adsorption characteristics of distillers dried grains with solubles (DDGS). Cereal Chem. 84:548-555.

Ganesan, V., Muthukumarappan, K., and Rosentrater, K. A. 2008. Sorption isotherm characteristics of dried distillers grain with solubles. Trans. ASABE 51:169-176.

Ganesan V., Rosentrater, K. A., and Muthukumarappan, K. 2009. Physical and flow properties of regular and reduced fat DDGS. Food Bioprocess Technol. 2:156-166.

Gibson, L. R., McCluskey, P. J., Tilley, K. A., and Paulsen, G. M. 1998. Quality of hard red winter wheat grown under high temperature conditions during maturation and ripening. Cereal Chem. 75:421-427.

Kingsly, A. R. P., and Singh, D. B. 2007. Drying kinetics of pomegranate arils. J. Food Eng. 79:741-744.

Law, C. L., Tasirin, S. M., and Daud, W. R. W. 2003. A new variable diffusion drying model for the second falling rate period of the paddy dried in a rapid bin dryer. Drying Technol. 21:1699-1718.

Madhiyanon, T., Soponronnarit, S., and Tia, W. 2002. A mathematical model for continuous drying of grains in a spouted bed dryer. Drying Technol. 20:587-614.

Menges, H. O., and Ertekin, C. 2006. Modelling of air drying of Hacihaliloglu-type apricots. J. Sci. Food Agric. 86:279-291.

Myers, H. R. 1986. Classical and Modern Regression Applications, 2nd Ed. Duxbury: Belmont, CA.

Polat, O. 1989. Through drying of paper. Ph.D. diss. McGill University: Montreal, Canada.

Renewable Fuels Association (RFA). 2010. Industry resources coproducts. Available at www.ethanolrfa.org/industry/resources/coproducts/.

Rock, M., and Schwedes, J. 2005. Investigations on the caking behaviour of bulk solids—Macroscale experiments. Powder Technol. 157: 121-127.

Rosentrater, K. A., and Muthukumarappan, K. 2006. Corn ethanol coproducts: Generation, properties, and future prospects. Int. Sugar J. 108:648-657.

Rosentrater, K. A., Flores, R. A., Richard, T. L., and Bern, C. J. 1999. Physical and nutritional properties of corn masa byproduct streams. Appl. Eng. Agric. 15:515-523.

Seber, G. A., and Wild, C. J. 1989. Nonlinear Regression. Wiley: New York.

Sharma, G. P., Prasad, S., and Datta, A. K. 2003. Drying kinetics of garlic cloves under convective drying conditions. J. Food Sci. Technol. 37:520-522.

Simal, S., Femenia, A., Garau, M. C., and Rosselló, C. 2005. Use of exponential, Page's and diffusional models to simulate the drying kinetics of kiwi fruits. J. Food Eng. 66:323-328.

Sogi, D. S., Shivhare, U. S., Garg, S. K., and Bawa, A. S. 2003. Water sorption isotherm and drying characteristics of tomato seeds. Biosyst. Eng. 84:297-301.

Speihs, M. J., Whitney, M. H., and Shurson, G. C. 2002. Nutrient database for distiller's dried grains with solubles produced from new ethanol plants in Minnesota and South Dakota. J. Anim. Sci. 80:2639-2645.

Tolaba, M. P., Aguerre, R. J., and Suárez, C. 1997. Modeling cereal grain drying with variable diffusivity. Cereal Chem. 74:842-845.

Wang, D. C., Fon, D. S., and Fang, W. 2004. Development of SAPGD—A simulation software regarding grain drying. Drying Technol. 22:609-625.

Zheng, X., and Lan, Y. 2007. Effects of drying temperature and moisture content on rice taste quality. Agric. Eng. Int.: CIGR J. 9(1):1-9. Available at http://www.cigrjournal.org/index.php/Ejounral/article/view/913.